Dalton Transactions

ROYAL SOCIETY OF CHEMISTRY

PAPER

View Article Online
View Journal | View Issue

Cite this: *Dalton Trans.*, 2020, **49**, 4315

Cu(I)–I coordination polymers as the possible substitutes of lanthanides as downshifters for increasing the conversion efficiency of solar cells†

Jesús López-Molina,[a] Cecilio Hernández-Rodríguez,[b] Ricardo Guerrero-Lemus,[b] Eugenio Cantelar,[c] Ginés Lifante,[c] Marta Muñoz[d] and Pilar Amo-Ochoa *[a,e]

Received 31st January 2020,
Accepted 25th February 2020

DOI: 10.1039/d0dt00356e

rsc.li/dalton

This study tries to provide new solutions to increase the efficiency of conversion of photons in solar cells, using photoluminescent Cu(I) coordination polymers (CPs) as possible alternative materials of lower cost, than those used today, based on lanthanides. The selected CP of chemical formula $[Cu(NH_2MeIN)I]_n$ (NH_2MeIN = methyl, 2-amino isonicotinate) absorbs in the utraviolet and emits in the visible region, being also easily nanoprocessable, by a simple and one-pot bottom-up approach. Nanofibers of this CP can be embedded in organic matrices such as ethyl vinyl acetate (EVA), forming transparent and homogenous films, with a thermal stability of up to approximately 150 °C. These new materials maintain the optical properties of the CP used as a dopant, ($[Cu(NH_2MeIN)I]_n$), with emission in yellow (570 nm) at 300 K, which is intensified when the working temperature is lowered. In addition, these materials can be prepared with varying thicknesses, from a few microns to a few hundred nanometers, depending on the deposition method used (drop casting or spin coating respectively). The study of their external quantum efficiency (EQE) found an increase in the UV range, which translates into an increase in the conversion efficiency. The optimal CP concentration is 5% by weight in order to not diminish the transparency of the composite material. The calculated cost on the possible incorporation of this material into solar cells shows a 50% decrease over the cost reported in similar studies based on the use of lanthanides.

Introduction

Huge scientific efforts have been made for several years for increasing the conversion efficiency of solar cells by converting photons from the UV spectral range, where the external quantum efficiency (EQE) of solar cells is low.[1] These efforts have been mostly based on the introduction of lanthanides[2] as downshifters directly into the bulk cell substrate[3] or on their surface as an additional layer.[4] This second procedure is prevailing at present because of the low cost, easiness and potential to be integrated into the photovoltaic (PV) module lamination process.[5] Moreover, recent works show that the integration of such downshifters can increase the efficiency of the standard Si-based solar cells by up to 0.31%, without optimizing the optics of the device.[6] Moreover, this absorbing capacity of UV radiation prevents the undesirable degradation of some of the constituents of solar cells, thereby improving the life time of photovoltaic cells and increasing the efficient potential of the solar cells in a useful manner. However, lanthanides are expensive, and a full range of alternative materials have been studied.[7] In this paper, we propose a photoluminescent coordination polymer (CP) based on Cu(I) as a possible sensitizer. From an economic point of view, copper is more abundant and less expensive than other metals, and luminescent CPs based on Cu(I) are cheaper than others based on Ag(I) or Au(I). In addition, these soft metals show high polarizability to establish stable covalent bonds with soft ligands such as halides. In this context, CPs based on Cu(I)–I double chains have been shown to be a subfamily with remarkable optical properties but, even more importantly, with very sensitive and flexible structures.[8] Thus, the structures

[a]*Facultad de Ciencias, Dpto. Química Inorgánica, Universidad Autónoma de Madrid 28049, Spain. E-mail: pilar.amo@uam.es*
[b]*Departamento de Física, Universidad de La Laguna, 38207 San Cristóbal de La Laguna, Spain*
[c]*Facultad de Ciencias, Dpto. Física de Materiales, Universidad Autónoma de Madrid 28049, Spain*
[d]*Departamento de Matemática Aplicada, Ciencia e Ingeniería de los Materiales y Tecnología Electrónica. Universidad Rey Juan Carlos, Madrid 28933, Spain*
[e]*Institute for Advanced Research in Chemistry (IAdChem), Universidad Autónoma de Madrid, Madrid 28049, Spain*

†Electronic supplementary information (ESI) available: Tables of crystallographic data, X-ray powder diffractograms, emission spectra and additional figures. See DOI: 10.1039/d0dt00356e

of these materials undergo slight structural changes under external physical and/or chemical stimuli, such as vapours, temperature and/or pressure, which significantly affect their physical properties, *e.g.* conductivity and/or emission.[9,10] In particular, the photoluminescence of copper(I) halides with organic nitrogen-donor ligands has been extensively studied for performance as chemical[11] or biological sensors.[12] Although coordination polymers have not acquired great relevance at the industrial level,[13] the possibility of creating composite materials using coordination polymers with an organic matrix, as, for example, ethyl vinyl acetate (EVA), can give rise to a new range of materials that retain the intrinsic optical properties of coordination networks.[9] The CP studied in this work $[CuI(NH_2\text{-MeIN})]_n$ (NH_2-MeIN = methyl, 2-amino isonicotinate) has an absorption band in the ultraviolet region and although it shows low emission at 25 °C, the intensity of the emission increases by lowering the temperature. In addition, this one-dimensional coordination polymer can be instantaneously nanoprocessed by bottom-up approximation, in a simple direct synthesis at room temperature, which will allow composite materials of nanometric thicknesses to be created with similar functionality and much lower cost. Therefore, the incorporation of Cu(I) coordination polymers of nanometric size in solar cells allows a new demand for innovative and intelligent materials to be introduced into the market as an alternative option to the rare earth monopoly.

Results and discussion

Synthesis of composite materials $[Cu(NH_2\text{-MeIN})I]_n$@EVA

The coordination polymer 1D-$[Cu(NH_2\text{-MeIN})I]_n$ (Fig. 1) has been successfully obtained in nanometric dimensions[9] by instantly direct synthesis between CuI and methyl-2-aminoisonicotinate (NH_2-MeIN) in a mixture of acetonitrile : ethanol at room temperature (sec. S1, Fig. S1†). This coordination polymer presents interesting optical properties that make it an excellent candidate for the study carried out in this work: (i) The CP shows emission in yellow at 300 K, which intensifies strongly when the temperature decreases (80 K)[9] as a result of an increase in its structural rigidity and, therefore, a constraint or decrease in its bond distances.[14]

In addition, the CP absorbs around 350 nm (ultraviolet) (Fig. S8†). These characteristics make it an interesting compound for the manufacture of new composite materials.

As solar panels must work outdoors under ambient conditions, their components must have a series of characteristics that allow it to withstand the weather. EVA has been chosen in the study due to its capacity of withstanding very extreme temperatures. In addition, it is highly transparent to allow solar energy to reach the photovoltaic cell without significant absorption and also has flexibility and high impact resistance to protect the cells from possible mechanical damages. Moreover, it is able to provide electrical insulation to avoid the risk of fire and has thermal stability, being the standard encapsulation material used in the photovoltaic industry.[15] All of these characteristics will extend the life of the panel, beyond 25 years, and protect it from external agents such as moisture or dust.

The manufacture of the composited materials at different proportions of the nano coordination polymers (5–30 wt%) was done dissolving the EVA in trichloroethylene (TCE) at 85 °C and over this solution, and different amounts (by weight) of $[Cu(NH_2\text{-MeIN})I]_n$ were added. Both components were mixed and dispersed by sonication tip (Fig. 2a). The X-ray powder diffraction and IR spectra of composite materials with different proportions of the CP (5–30 wt%) show that the synthesis conditions used for the creation of these materials do

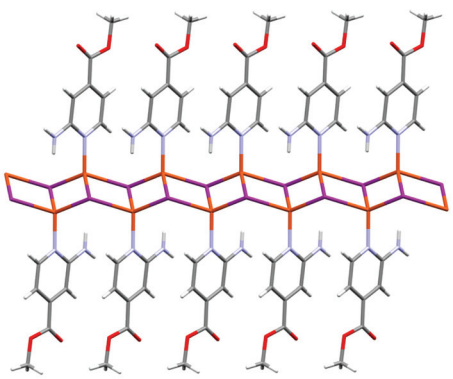

Fig. 1 Fragment of the crystal structure of the CP **1D-$[Cu(NH_2\text{-MeIN})I]_n$** solved by single-crystal X-ray diffraction at 296 K.[9] Orange: Cu, purple: I, blue: N, black: C, red: O, grey: H.

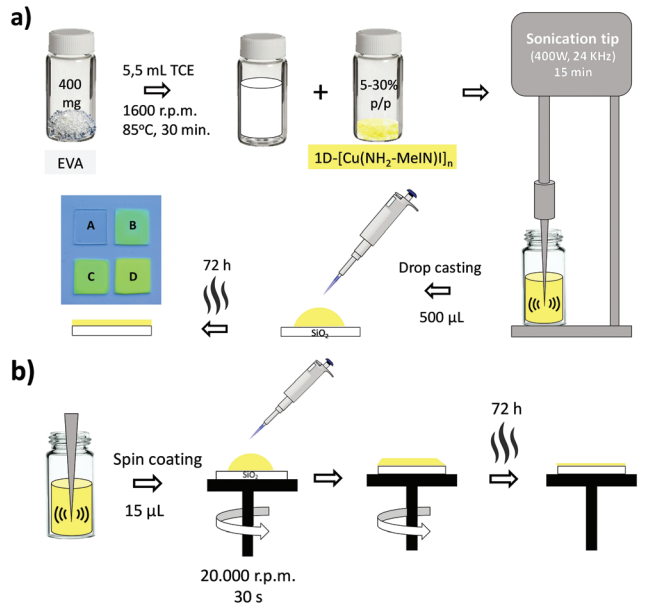

Fig. 2 (a) Schematic synthesis to prepare thin films of **$[Cu(NH_2\text{-MeIN})I]_n$@EVA (5–30 wt%)** and deposition over SiO_2 surfaces by drop casting. (b) Schematic procedure of **$[Cu(NH_2\text{-MeIN})I]_n$@EVA (5–30 wt%)** composites deposited on SiO_2 surfaces by spin-coating.

not alter the structure of the CP within the organic matrix (EVA) (Fig. S4 and S5†).

The homogeneity of the composite material [Cu(NH_2-MeIN)I]$_n$@EVA was also studied by SEM-EDX. In the material prepared only with EVA (Fig. S9A†), a high C and O content is identified, corresponding to the elemental composition of EVA organic polymers. After incorporating 5, 10 and 15% (wt) of the coordination polymer [Cu(NH_2-MeIN)I]$_n$ (Fig. S9B–D†), the spectrum identified a constant ratio of 1 : 1 (Cu : I) content in each hybrid material manufactured. In addition, TXRF made over **[Cu(NH_2-MeIN)I]$_n$@EVA-5%** corroborates a homogeneous distribution of CPs (Fig. S10†).

The thickness of composite materials is regulated by two different deposition methods. In the case of requesting micrometric thickness films, the deposition of these suspensions on SiO_2 was carried out by drop casting, obtaining films of around 2.0 × 2.0 × 0.2 mm dimensions (Fig. S23A–E†). If the thickness of the films is required to reach a nanometer or submicrometer scale, spin coating is used, obtaining films of around 150 nm thickness (Fig. 3).

Composite materials [Cu(NH_2-MeIN)I]$_n$@EVA: thermal stability

As shown in Fig. 4 and Fig. S6,† the thermogravimetric analysis of EVA, 1D-[Cu(NH_2-MeIN)I]$_n$ and [Cu(NH_2-MeIN)I]$_n$@EVA, respectively, have been carried out, in order to know the thermal stability of the CP after embedding it in the EVA organic matrix. The EVA thermogram shows two stages of thermal decomposition. The first mass loss of 19%, observed from 300 to 400 °C, corresponds to the deacetylation of the vinyl group, which results in the production of acetic acid in the gaseous state and the formation of carbon–carbon double bonds throughout the polymer chain. The remaining mass loss, observed from 400 to 500 °C, corresponds to the thermo-oxidation of the unsaturated chains and to the volatilization by rupture of the double bonds.[16] The thermogram of 1D-[Cu(NH_2-MeIN)I]$_n$, shows a first thermal decomposition from 150 to 250 °C with a mass loss of 44%, corresponding to the decomposition of methyl-2-aminoisonicotinate (NH_2-MeIN). The second loss takes place from 400 to 700 °C, corresponding to the remains of volatile copper–iodine compounds. The thermogravimetric analysis of [Cu(NH_2-MeIN)I]$_n$@EVA-5–15% (Fig. 4, S6c–e and S7†) shows that the incorporation of the coordination polymer into EVA does not affect the thermal stability of the reinforcement matrix.

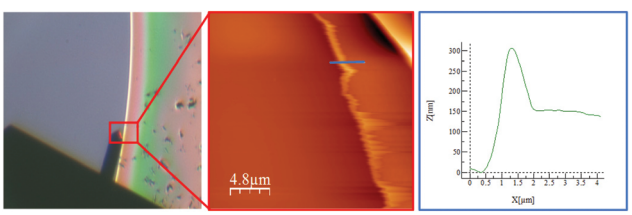

Fig. 3 AFM images showing sub-micrometer thickness of the **[Cu(NH_2-MeIN)I]$_n$@EVA-5 wt%** composite film, deposited on SiO_2 surfaces by spin-coating.

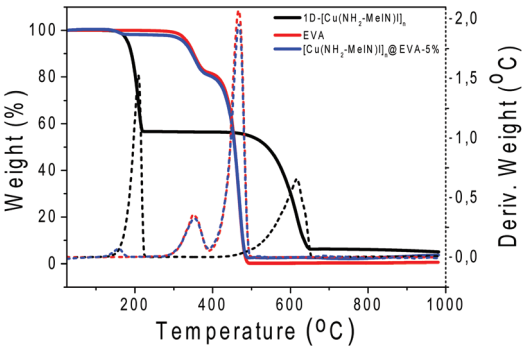

Fig. 4 Thermogravimetric analysis coupled to differential thermal analysis (TGA-DTA) of **1D-[Cu(NH_2-MeIN)I]$_n$** (black line), **EVA** (red line) and **[Cu(NH_2-MeIN)I]$_n$@EVA-5%** thin films (blue line) in a temperature range from 25 to 1000 °C, under nitrogen gas at a flow rate of 90 mL min^{-1} and a heating rate of 10 °C min^{-1}, in a range temperature from 25 to 1000 °C.

Further, the first thermal decomposition of the composite material, around 150 °C, is close to the maximum thermal stability limit necessary for the integration process in photovoltaic (PV) minimodules.[17] Then, this study shows that [Cu(NH_2-MeIN)I]$_n$@EVA thin films could be incorporated in any step of the minimodule assembly, since this process is usually carried out at temperatures close to 150 °C.

Composite materials [Cu(NH_2-MeIN)I]$_n$@EVA: luminescence properties

The compound 1D-[Cu(NH_2-MeIN)I]$_n$ selected to be introduced into the organic matrix (EVA) has temperature-dependent luminescent behaviour.[9] At 300 K, and after excitation with λ_{exc} = 365 nm, [Cu(NH_2-MeIN)I]$_n$ has a weak yellow emission with an asymmetric band centred at λ_{em} = 550 nm, while upon cooling the temperature from 300 to 80 K, exhibits a progressive increase in its emission intensity without shifting of the main band. This process is reversible and, thus, warming up the materials from 80 K to 300 K produces a gradual recovery of their initial properties, which makes it a temperature-dependent luminescent material.[9] This increase in emission intensity with the decrease in temperature can be explained based on the crystalline structure solved at 296 and 110 K by single-crystal X-ray diffraction (Table S1†). Although the unit cell coincides with both temperatures, the flexibility of the double chains Cu(I)–I makes the coordination polymer behave like a true 'molecular spring', given that the distances Cu–I and Cu···Cu (Å) are shortened and the angles I···Cu···I (°) are contracted when the temperature decreases (Table S2†), due to an increase in the structural rigidity of the compound. The emission centered around 550–570 nm can be most likely due to a mixed iodine-to-ligand and metal-to-ligand charge transfer (IL/ML(CT) [3(I + M)LCT].[18]

When 1D-[Cu(NH_2-MeIN)I]$_n$ is embedded in EVA, a naked eye experiment of [Cu(NH_2-MeIN)I]$_n$@EVA under UV lamp (λ_{exc} = 312 nm) at 80 K showed that [Cu(NH_2-MeIN)I]$_n$@EVA-15% film deposited in SiO_2 emits in the yellow region very inten-

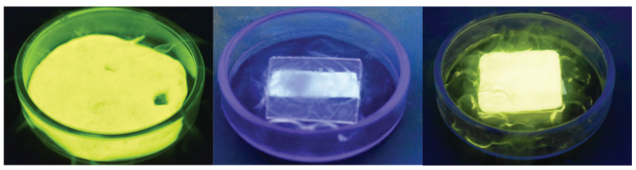

Fig. 5 Emission in a naked eye experiment under a UV lamp (λ_{exc} = 312 nm) at 80 K of **1D-[Cu(NH$_2$-MeIN)I]$_n$** (left), **EVA** (middle) and **[Cu(NH$_2$-MeIN)I]$_n$@EVA-15%** (right) composite films deposited on SiO_2 surfaces.

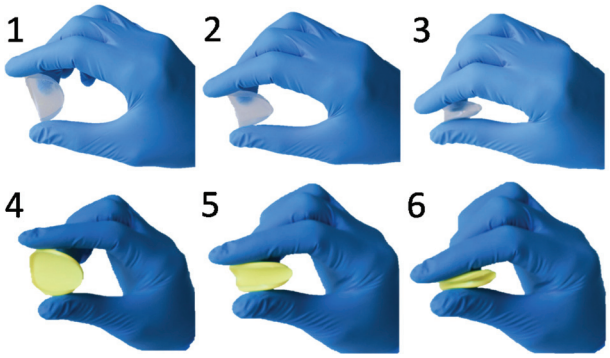

Fig. 7 Flexibility degree in a naked-eye experiment under visible light at 296 K of **EVA** (first row: images 1–3) and **[Cu(NH$_2$-MeIN)I]$_n$@EVA-30%** thin films (second row: images 4–6).

sely, showing that the new composite materials retain the luminescent properties of the coordination polymer, thus creating a photoluminescent composite with temperature response (Fig. 5 and Fig. S18–20†).

The emission spectra of the new composite material ([Cu(NH$_2$-MeIN)I]$_n$@EVA-5–30%) (λ_{exc} = 400 nm) have a very weak band (low intensity) at room temperature, which increases as the temperature drops, reaching a maximum around 570 nm at 80 K (Fig. 6). This behavior is analogous in all composite materials regardless of the concentration of the added CP (5, 10, 15, and 30%) (Fig. S11–20†). This process is reversible and thus warming up the materials from 80 K to 300 K produces a gradual recovery of their initial properties. These results show, as we have already mentioned, that the new composite materials retain the optical properties of the selected CP.

Composite materials [Cu(NH$_2$-MeIN)I]$_n$@EVA: transparency and mechanical properties

One of the advantages of preparing composite materials is that their manufacturing involves an improvement in the mechanical properties of the coordination polymer. As shown in Fig. 7 and S21,† the micrometric thickness of the film prepared only with the EVA organic matrix allows to obtain a flexible and transparent material. The degree of processability is maintained even after embedding 30% of [Cu(NH$_2$-MeIN)I]$_n$ in the organic matrix (Fig. 7 (4–6)), retaining in any of the cases almost the original flexibility of EVA. However, the transparency degree in the film Cu(I)–EVA decreases dramatically when the content of the coordination polymer in the organic matrix was increased.

The UV/Visible absorption study (Fig. S22†) shows that the opacity of the prepared composite materials increases with the increase in the concentration of the coordination polymer on EVA. The film made only with EVA, used as a reference target, almost does not absorb radiation in the range of 190–1100 nm, due to its high transparency. When 5% of 1D-[Cu(NH$_2$-MeIN)I]$_n$ is incorporated into EVA, the composite absorbs almost all the incident radiation. A higher weight percentage of the coordination polymer selected (10, 15 and 20 wt%) shows that the absorbance signal in the composite materials is saturated because the opacity of the film is becoming more marked. In principle, these results presuppose an inconvenience for external quantum efficiency (EQE) measures, since the transparency of the films is an indispensable requirement for the measures to be legible.

The tensile test curves of the [Cu(NH$_2$-MeIN)I]$_n$@EVA composites are plotted in Fig. 8. The tensile test was also per-

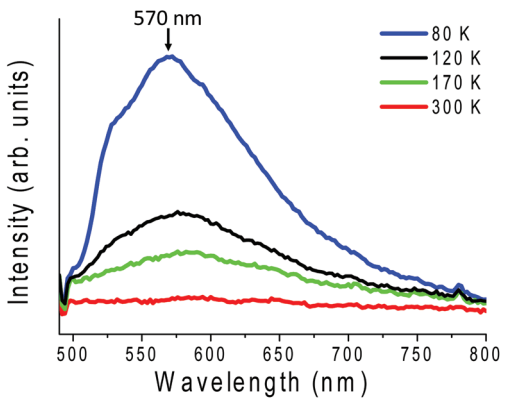

Fig. 6 Emission spectrum of **[Cu(NH$_2$-MeIN)I]$_n$@EVA-5%** after excitation at 400 nm, at different temperatures, from 298 K (red line) to 80 K (blue line).

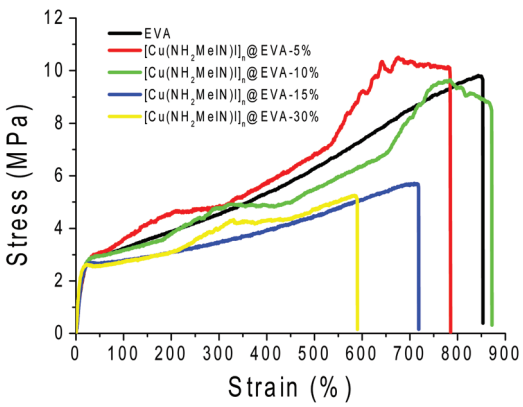

Fig. 8 Stress–strain curves of pristine EVA and [Cu(NH$_2$-MeIN)I]$_n$@EVA composites.

formed on the pristine EVA polymer for comparison. From the stress–strain curves, we can see the influence of different concentrations of $[Cu(NH_2\text{-MeIN})I]_n$ reinforcement on the EVA mechanical properties.

The load increases linearly with a high slope at first, and then it increases more gradually. The mechanical properties are listed in Table S4.† Films fabricated with the highest concentration of nanofibers show a very slightly higher rigidity directly connected with this increment in the elastic modulus value.

The results revealed that the incorporation of $[Cu(NH_2\text{-MeIN})I]_n$ decreases the fracture strength value (σ_u) proportionally to the $[Cu(NH_2\text{-MeIN})I]_n$ content, achieving the lowest values of fracture strength of nearly 5.72 and 5.51 MPa at 15% and 30%, respectively (Table S4†). That seems to be related to a weak interaction at the matrix–reinforcement interface in the composite. At high concentrations, 10%, 15% and 30% (wt), nanofibers can probably form agglomerates decreasing their interactions with the polymeric matrix. However, fracture strain values decrease with the increment in the concentration of the reinforcement, achieving a minimum value, 603 %, at the highest concentration 30% (wt) with a wide range of variability, mainly due to the poor adhesion between the nano-reinforce and the EVA matrix. The addition of different amounts of nanofibers to the EVA matrix does not alter the elastic modulus value of the nanocomposite. This can also be due to the weak interaction between the EVA matrix and $[Cu(NH_2\text{-MeIN})I]_n$ reinforcement. Essentially, the tensile test shows that for up to 5% by weight compositions of the CP in the EVA, it does not suffer any drastic change in its fracture strength and fracture strain, nor in the elastic modulus. Therefore, this composition which is the ideal, in terms of transparency and EQE (see below), would also maintain the mechanical properties of the matrix.

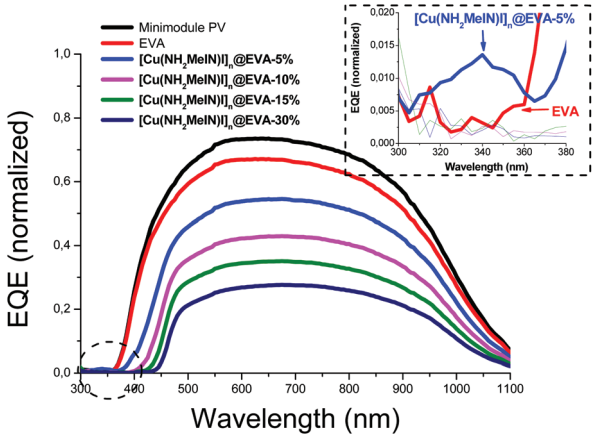

Fig. 9 External Quantum Efficiency (EQE) spectrum collected for **EVA** (red line), **$[Cu(NH_2\text{-MeIN})I]_n$@EVA-5%** (light blue line), **$[Cu(NH_2\text{-MeIN})I]_n$@EVA-10%** (pink line), **$[Cu(NH_2\text{-MeIN})I]_n$@EVA-15%** (green line) and **$[Cu(NH_2\text{-MeIN})I]_n$@EVA-30%** (dark blue) thin-films deposited in the Si photovoltaic minimodule, in a wavelength range from 300 to 1100 nm at room temperature. Inset figure: Extension of the wavelength zone between 300 and 380 nm.

Composite materials $[Cu(NH_2\text{-MeIN})I]_n$@EVA: external quantum efficiency (EQE) measurement

The influence of the composite material on the solar reference PV cell is evaluated by EQE, that is, by the fraction of incident photons that reach the solar cell and produce an electron–hole pair in the external circuit under short-circuit conditions.[19] The EQE spectra, exposed in Fig. 9, show values for a PV minimodule covered by glass and EVA and compared, under the same conditions, with the same minimodule placing the different luminescent films embedded in EVA at different concentrations. When the $[Cu(NH_2\text{-MeIN})I]_n$@EVA-5% film is incorporated into the Si photovoltaic minimodule, a slight increase in the UV spectral range (300–380 nm) is observed with respect to the PV mini-module covered only with the bare glass, whose EQE value is close to zero. The lowering of EQE in the visible region by incorporating the film into the photovoltaic minimodule (substantial in the short wavelength region of the visible range) is due to the increase in opacity of the EVA + Cu-based film when the film concentration is increased. Of all the luminescent films deposited, $[Cu(NH_2\text{-MeIN})I]_n$@EVA-5% is the only one that shows an appreciable increase in the value of EQE in the UV region also because, below this percentage, the conversion process is negligible, and above this percentage, the increase in opacity also affects the UV spectral range, avoiding the transmittance of the shifted photons to the solar cell. Moreover, it is important to mention that the integration of the downshifter has not been optically optimized by encapsulating it to the minimodule. This is due to the need to use the same minimodule for appropriately comparing the EQE spectra with the different samples. Nevertheless, since an increase in the value of EQE in the UV region translates into an increase in conversion efficiency, it becomes clear that $[Cu(NH_2\text{-MeIN})I]_n$ is an active species with an interesting potential for its application in solar cells, since it is capable of moving the photons of the incident radiation (UV region) to longer wavelengths, where the Si solar cell shows higher conversion efficiency (visible region), avoiding absorption and reflection losses of the photons, as well as parasitic absorptions,[19–21] and also preventing the undesirable degradation of EVA, thus improving the useful life of photovoltaic cells and increase the efficiency of the solar cell.[22,23] Thus, the values of EQE are expected to increase in the UV range as the concentration of $[Cu(NH_2\text{-MeIN})I]_n$ increases in the organic matrix to the limit of solubility or luminescence saturation, as it has been described elsewhere.[17,20] It is necessary to emphasize that the thickness of the luminescent film affects the EQE result, since it is linked to an increase in absorption in the UV range and, to a lesser extent, a lower transmittance of the film. This affection can be considered very similar to variations in the active species concentration in the film. In future works we will define a protocol to optimize the thickness and active species concentration in the film, also taking into account that

the deposition procedure must remain simple to be competitive for being adapted to the PV industry.

Composite materials $[Cu(NH_2\text{-MeIN})I]_n$@EVA: industrial cost estimation

Based on the increase in energy efficiency registered in the photovoltaic cell after incorporating the luminescent films, as well as the high processability and the low environmental impact of manufacturing these novel copper(I)-based composite materials, the additional cost has been calculated, which involves the incorporation of these films into new solar cells.

To date, luminescent active species based on rare earths have been taken into account as Eu^{3+} (ref. 6, 19 and 24) or Gd^{3+},[6] or dyes.[25] In this work, the incorporation of a transition metal d^{10} as a metallic center, copper in this case, makes possible to considerably reduce the costs if the expected increase in EQE in the UV range is appreciable and the decrease in EQE at larger wavelengths due to increases in the opacity is avoided. The current price in the copper iodide wholesale market is around 8 € per kg, and the cost of the organic ligand is 0.90 € per kg. Taking into account the stoichiometry, the synthesis yield and the solvent expense, the price involved in the synthesis of the coordination polymer $[Cu(NH_2\text{-MeIN})I]_n$ is 9.09 € per kg. Knowing that the cost of the organic matrix (EVA) is 1.5 € per kg and that to make a composite film of EVA and $[Cu(NH_2\text{-MeIN})I]_n$ at 5% by weight, 20.0 mg of coordination polymer is needed, the global expense to manufacture a sheet of micrometric thickness is 0.041 € per m^2, a half of the expected costs reported with lanthanides in the literature.[26]

Conclusion

Based on the requirements to obtain a response in the photovoltaic cell, coordination polymers (CPs) based on CuI with pyridine derivatives can be an interesting new family of compounds, that thanks to their optical properties and their low cost, compared with the rare earth, should be used as substitutes of lanthanides as downshifters for increasing the conversion efficiency of solar cells.

In this work, 1D-$[Cu(NH_2\text{-MeIN})I]_n$ has been selected as an active species, since it absorbs in the ultraviolet region and present yellow emission. In addition, its nanoprocessing is very simple thanks to its high insolubility in the reaction medium. For these reasons, it has been selected for the creation of new micro or ultrathin (nano) composite material films with EVA as an organic matrix. The new composite materials maintain the optical properties of the CP and at low concentrations of the CP (5%) also maintain a high degree of transparency; the EVA mechanical properties, even the thermal decomposition, are close to the maximum thermal stability limit necessary for the integration process in photovoltaic minimodules. In addition, $[Cu(NH_2\text{-MeIN})I]_n$@EVA-5% shows an appreciable increase in the value of EQE in the UV region.

This study opens the possibility of designing new cheaper composite materials based on this wide family of CuI double-chain CPs, selecting those that present in addition to UV absorption, high emission intensity in the visible region at 300 K. The degree of transparency can be modified playing with the thickness and the amount of the CP on the composite materials, among other factors.

Experimental

Materials and methods

All reagents and solvents purchased were used without further purification. The reagents used in the synthesis, copper(I) iodide and methyl-2-aminoisonicotinate, were purchased from Sigma Aldrich (CAS: 7681-65-4 and 14667-47-1). The solvents used in the synthesis, acetonitrile and ethanol, were purchased from VWR with HPLC purification grade. Poly-(ethylene vinyl acetate) (EVA) was purchased from Sigma-Aldrich, with 25% vinyl acetate and 400–900 ppm of BHT as an inhibitor. Trichloroethylene (TCE) was purchased from Panreac and is stabilized in EtOH. TCE was used to improve the dissolution of hot EVA.

The dispersion of the coordination polymer in the EVA organic matrix was carried out using a sonication tip Hielscher UP400S (power: 400 W, frequency: 24 kHz). IR spectra were recorded using a PerkinElmer 100 spectrophotometer with a universal attenuated total reflection (ATR) sampling accessory from 4000 to 650 cm^{-1}. Elemental analyses were performed using a LECO CHNS-932 Elemental Analyzer. Powder X-ray diffraction data were collected using a Diffractometer PANalytical X'Pert PRO equipped with a $\theta/2\theta$ primary monochromator and an X'Celerator fast detector and monochromator, 1° for $K_{\alpha 1}$. The samples have been analyzed with scanning $\theta/2\theta$, from 3–60 degrees, with an angular increase of 0.0167 and a time per increment of 100 s. Thermogravimetric analyses (TGA) were carried out using a TA Instruments Q500 thermobalance oven with a Pt sample holder. Experiments were carried out under nitrogen gas at a flow rate of 90 mL min^{-1} and a heating rate of 10 °C min^{-1}, in a range temperature from 25 to 1000 °C. The transparency of the hybrid materials was measured by UV-visible absorption, using an Agilent 8452 diode array spectrophotometer over the solid samples at room temperature. The spectra were recorded in a wavelength range from 190 to 1100 nm. Scanning electron microscopic (SEM) images were taken using a JMS 6335F electron microscope, applying an electron beam of 300 μA intensity and 15.0 kV potential, at a pressure of 10^{-7} Pa. After sample preparation, the films were metallized with a 15 nm thick Au layer, at a pressure of 10^{-3} Pa. SEM-EDX images and EDX spectra were recorded using a Hitachi S-3000N microscope with an ESED coupled to an INCAx-sight EDX analyser. For this technique, the samples were metallized with a gold layer of 15 nm, under a pressure of 10^{-3} Pa. Atomic force microscopic images were obtained using a Nanotec Electronica microscope, at room temperature and in an open atmosphere, using Olympus canti-

levers with a constant nominal force of 0.75 N m^{-1}. Images were processed by the use of the WSxM program. The analysis by TXRF was performed using a TXRF 8030C spectrometer (Cameca, France), equipped with a 3 kW X-ray tube with a Mo/W alloy anode with a double-W/C multilayer monochromator, adjusted to obtain an excitation energy of 17.4 keV (Mo-K_α), for Cu and I evaluation, and a Si(Li) detector with an active area of 80 mm^2 with a resolution of 150 eV at 5.9 keV (Oxford Instruments, England). The measurements were performed working at 50 kV, and the intensity was adjusted automatically, so that a count rate of about 8500 cps was achieved. A fixed acquisition time of 500 s was used. The photovoltaic (PV) device where the downshifter is placed is a PV mini module based on a single p-type mc-Si solar cell (non-textured and with a SiNx antireflection coating optimized at 600 nm) encapsulated in a standard solar glass and showing a 16% conversion efficiency. A standard EQE setup based on a 100 W Xe arc lamp, a monochromator and a digital lock-in amplifier was used. The PV mini-module is fixed in the EQE setup to assure the reproducibility of results between samples. Moreover, the glass substrates with EVA and with or without the downshifter are fixed on top of the mini-module.

Excitation and emission spectra. The excitation spectra were performed using a 450 W Xe lamp attached to a Digikröm CM-110 monochromator with 110 mm focal length. The thermal dependence of the luminescence emission spectra of films was analyzed using an ARC Spectrapro 500-I monochromator with 500 mm focal length, and then detected with a photo-multiplier tube, where a long pass filter was placed at the entrance slit of the monochromator to block the excitation light. Measurements at variable temperature were carried out using an Oxford Cryostat Optistat DN.

Synthetic procedures

Synthesis of 1D-[Cu(NH_2-MeIN)I]$_n$. The synthesis procedure of the coordination polymer (CP), as well as its structural description, has been reported previously.[9] The CP was obtained by a stoichiometric reaction between CuI (100 mg, 0.53 mmol) and methyl-2-aminoisonicotinate (81 mg, 0.53 mmol) at 25 °C and under magnetic stirring (500 rpm), using a mixture of acetonitrile : ethanol (1 : 1) in the minimum amount possible to facilitate the instantaneous precipitation of the reaction product. A pale-yellow solid is immediately formed, filtered off, washed with acetonitrile (2 × 5 mL), ethanol (2 × 5 mL) and diethyl ether (2 × 3 mL), and dried in vacuum. Single crystals were formed upon standing the mother yellow solution at 25 °C for 72 h (yield: 85 mg; 50% based on Cu). Elemental analysis calcd (%) for $C_7H_8CuIO_2N_2$: C 24.52, H 2.34, N 8.17; found: C 24.96, H 2.34, N 8.07; IR selected data (ATR): n (cm^{-1}) = 3450 (s), 3345 (s), 3186 (w), 3078 (w), 2992 (w), 2945 (w), 2845 (w), 1788 (w), 1716 (vs), 1634 (vs), 1603 (m), 1560 (vs), 1489 (w), 1448 (vs), 1432 (s), 1346 (m), 1308 (vs), 1270 (vs), 1249 (s), 1123 (s), 999 (s), 900 (m), 830 (w), 816 (m), 762 (vs), 737 (m), 697 (w). The powder X-ray diffraction (PXRD) data of the compound confirmed the purity of both the crystals and solid.

Preparation of composite thin film [Cu(NH_2-MeIN)I]$_n$@EVA

Ethyl vinyl acetate (EVA) polymer was doped with coordination polymer 1D-[Cu(NH_2-MeIN)I]$_n$ in 5, 10, 15 and 30% (wt). First, 0.400 g EVA was dissolved in 5.5 mL of trichloroethylene (TCE) at 85 °C for 30 minutes, under magnetic stirring (1600 rpm). Then, over this solution, 20.0, 40.0, 60.0, 80.0 and 120.0 mg of [Cu(NH_2-MeIN)I]$_n$ were added, respectively. Both the components were mixed and dispersed by sonication for 15 minutes at 25 °C (65% amplitude). By drop-casting, 500 μL of the resulting homogeneous dispersion was deposited on SiO_2 surfaces (20 × 20 × 2 mm) and dried in air for 48 h to remove TCE by low evaporation. This solution amount is enough to obtain films of micrometric thickness that completely cover the glass, which are optimum for the EQE experiments. Finally, the glass is directly placed on a PV minimodule, and illuminated for measuring the external quantum efficiency (EQE). The rest of the suspension is deposited in a Petri dish to obtain a film that allows the structural characterization of the composite thin film. IR, PXRD, TGA, SEM-EDX and emission spectral data showed the presence of [Cu(NH_2-MeIN)I]$_n$ in the films.

Preparation of composite sub-micrometer-thin film [Cu(NH_2-MeIN)I]$_n$@EVA

Herein, 15 μL of the dispersed material was supported on SiO_2 surfaces by spin-coating for 30 seconds at 20 000 rpm and dried with an argon flow for 3 minutes, obtaining a sheet of nanometer thickness which was confirmed by AFM (Fig. 3).

Mechanical characterization of film [Cu(NH_2-MeIN)I]$_n$@EVA

Tensile tests were performed using a MTS Alliance RT/5 testing machine (URJC, LATEP) equipped with a 500 N load cell at 23 °C and 50% humidity, according to the method 35 PP (ISO 527)_5A SIN. For each condition, at least three samples of each concentration were tested at a strain rate of 10 mm min^{-1}. The films were cut with a CEAST die cutting machine in dumbbell shape, 13 × 1.9 mm (Fig. S24†), and the thickness, controlled by the processing step, was close to 1 mm.

The initial separation between clamping jaws (l_0) was 20 mm and at least three samples of [Cu(NH_2-MeIN)I]$_n$@EVA composites with each concentration were tested. Force (F) and displacement (Δl) data for each test were obtained, and then converted to stress–strain using equations (1) and (2).

$$\sigma = \frac{F}{A_0} \quad (1)$$

$$e = \frac{\Delta l}{l_0} \quad (2)$$

The Young modulus (E) gives the relationship between stress (σ) and strain (e), which has been estimated using eqn (3):

$$\sigma = E \cdot e \quad (3)$$

Conflicts of interest

There are no conflicts to declare.

Acknowledgements

This article has been funded by the Spanish Ministerio de Economía y Competitividad (and the current Ministerio de Ciencia, Innovación y Universidades) (MAT2016-75883-C2-2-P, MAT2016-75716-C2-2-R and RTI2018-095563-B-100). This article is dedicated to J. J. Amo-Mora.

Notes and references

1 C. Strümpel, M. McCann, G. Beaucarne, V. Arkhipov, A. Slaoui, V. Švrček, C. del Cañizo and I. Tobias, *Sol. Energy Mater. Sol. Cells*, 2007, **91**, 238.
2 (*a*) S. G. Dunning, A. J. Nuñez, M. D. Moore, A. Steiner, V. M. Lynch, J. L. Sessler, B. J. Holliday and S. M. Humphrey, *Chem*, 2017, **2**, 579; (*b*) I. A. Ibarra, T. W. Hesterberg, J. S. Chang, J. W. Yoon, B. J. Holliday and S. M. Humphrey, *Chem. Commun.*, 2013, **49**, 7156.
3 M. J. Keevers and M. A. Green, *J. Appl. Phys.*, 1994, **75**, 4022.
4 Z. Chen, G. Wu, H. Jia, K. Sharafudeen, W. Dai, X. Zhang, S. Zeng, J. Liu, R. Wei, S. Lv, G. Dong and J. Qiu, *J. Phys. Chem. C*, 2015, **119**, 24056.
5 T. Monzón-Hierro, J. Sanchiz, S. González-Pérez, B. Gonzalez-Diaz, S. Holinski, D. Borchert, C. Hernández-Rodríguez and R. Guerrero-Lemus, *Sol. Energy Mater. Sol. Cells*, 2015, 187.
6 R. Guerrero-Lemus, J. Sanchiz, M. Sierra-Ramos, I. Martin, C. Hernández Rodríguez and D. Borchert, *Sens. Actuators, A*, 2018, **271**, 60.
7 X. Huang, S. Han, W. Huang and X. Liu, *Chem. Soc. Rev.*, 2013, **42**, 173.
8 (*a*) J. Troyano, J. Perles, P. Amo-Ochoa, F. Zamora and S. Delgado, *CrystEngComm*, 2016, **18**, 1809; (*b*) J. Troyano, J. Perles, P. Amo-Ochoa, J. I. Martínez, M. Concepción Gimeno, V. Fernández-Moreira, F. Zamora and S. Delgado, *Chem. – Eur. J.*, 2016, **22**, 18017; (*c*) K. Hassanein, J. Conesa-Egea, S. Delgado, O. Castillo, S. Benmansour, J. I. Martinez, G. Abellan, C. J. Gomez-Garcia, F. Zamora and P. Amo-Ochoa, *Chem. – Eur. J.*, 2015, **21**, 17282; (*d*) K. Hassanein, P. Amo-Ochoa, C. J. Gomez-Garcia, S. Delgado, O. Castillo, P. Ocon, J. I. Martinez, J. Perles and F. Zamora, *Inorg. Chem.*, 2015, **54**, 10738.
9 J. Conesa-Egea, N. Nogal, J. I. Martínez, V. Fernández-Moreira, U. R. Rodríguez-Mendoza, J. González-Platas, C. J. Gómez-García, S. Delgado, F. Zamora and P. Amo-Ochoa, *Chem. Sci.*, 2018, **9**, 8000.
10 G. K. Kole and J. J. Vittal, *Chem. Soc. Rev.*, 2013, **42**, 1755.
11 Z. Hu, B. J. Deibert and J. Li, *Chem. Soc. Rev.*, 2014, **43**, 5815.
12 P. Amo-Ochoa and F. Zamora, *Coord. Chem. Rev.*, 2014, **276**, 34.
13 U. Mueller, M. Schubert, F. Teich, H. Puetter, K. Schierle-Arndt and J. Pastré, *J. Mater. Chem.*, 2006, **16**, 626.
14 B. Valeur and M. N. Berberan-Santos, Front Matter, in *Molecular Fluorescence: Principles and Applications*, Wiley-VCH Verlag GmbH & Co, 2nd edn, 2012.
15 E. Klampaftis and B. S. Richards, *Prog. Photovoltaics*, 2011, **19**, 345.
16 S. Peeterbroeck, M. Alexandre, R. Jérôme and P. Dubois, *Polym. Degrad. Stab.*, 2005, **90**, 288.
17 R. Guerrero-Lemus, J. Sanchiz, M. Sierra-Ramos, I. R. Martín, C. Hernández-Rodríguez and D. Borchert, *Sens. Actuators, A*, 2018, **271**, 60.
18 L. Yang, D. R. Powell and R. P. Houser, *Dalton Trans.*, 2007, 955.
19 S. González-Pérez, J. Sanchiz, B. González-Díaz, S. Holinski, D. Borchert, C. Hernández-Rodríguez and R. Guerrero-Lemus, *Surf. Coat. Technol.*, 2015, **271**, 106.
20 T. Fix, A. Nonat, D. Imbert, S. Di Pietro, M. Mazzanti, A. Slaoui and L. J. Charbonnière, *Prog. Photovoltaics*, 2016, **24**, 1251.
21 G. Zucchi, V. Murugesan, D. Tondelier, D. Aldakov, T. Jeon, F. Yang, P. Thuéry, M. Ephritikhine and B. Geffroy, *Inorg. Chem.*, 2011, **50**, 4851.
22 A. W. Czanderna and G. J. Jorgensen, *AIP Conf. Proc.*, 1997, **394**, 295.
23 M. Aklalouch, A. Calleja, X. Granados, S. Ricart, V. Boffa, F. Ricci, T. Puig and X. Obradors, *Sol. Energy Mater. Sol. Cells*, 2014, **120**, 175.
24 B. González-Díaz, M. Sierra-Ramos, J. Sanchiz and R. Guerrero-Lemus, *Sens. Actuators, A*, 2018, **276**, 312.
25 E. Klampaftis, M. Congiu, N. Robertson and B. S. Richards, *IEEE J. Photovoltaics*, 2011, **1**, 29.
26 T. Monzón-Hierro, J. Sanchiz, S. González-Pérez, B. González-Díaz, S. Holinski, D. Borchert, C. Hernández-Rodríguez and R. Guerrero-Lemus, *Sol. Energy Mater. Sol. Cells*, 2015, **136**, 187.

